Journal Pre-proofs

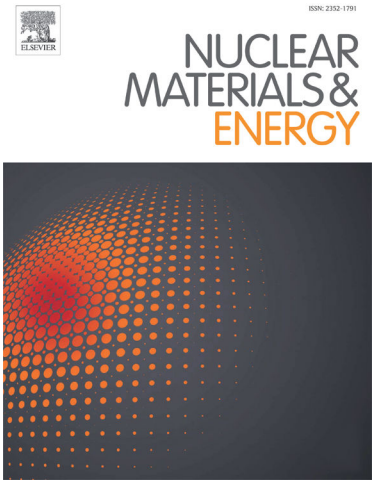

Long-term thermal stability of biphasic Li_4SiO_4-Li_2TiO_3 EU reference tritium breeder ceramics enriched in Li-6

Julia Leys, Thomas Bergfeldt, Oliver Leys, Regina Knitter

PII: S2352-1791(25)00074-2
DOI: https://doi.org/10.1016/j.nme.2025.101932
Reference: NME 101932

To appear in: *Nuclear Materials and Energy*

Received Date: 3 February 2025
Revised Date: 25 March 2025
Accepted Date: 6 April 2025

Please cite this article as: J. Leys, T. Bergfeldt, O. Leys, R. Knitter, Long-term thermal stability of biphasic Li_4SiO_4-Li_2TiO_3 EU reference tritium breeder ceramics enriched in Li-6, *Nuclear Materials and Energy* (2025), doi: https://doi.org/10.1016/j.nme.2025.101932

Long-term thermal stability of biphasic Li_4SiO_4-Li_2TiO_3 EU reference tritium breeder ceramics enriched in Li-6

Julia Leys*,julia.leys@kit.edu, Thomas Bergfeldt, Oliver Leys, Regina Knitter

Karlsruhe Institute of Technology (KIT), Institute for Applied Materials (IAM), Karlsruhe, Germany

*Corresponding author.

Highlights

- Experiment on long-term thermal stability (up to 60 d) of tritium breeder pebbles
- Advanced Ceramic Breeder (ACB) pebbles with 60–90 at% lithium-6 enrichment
- Biphasic pebbles remain chemically and mechanically stable at 900 °C

Abstract

The long-term thermal stability of Advanced Ceramic Breeder (ACB) pebbles was investigated in an annealing experiment at 700 and 900 °C in He + 0.1 vol% H_2 gas atmosphere for up to 60 days. Four batches of biphasic ACB pebbles, consisting of Li_4SiO_4 with additions of 30 and 35 mol% Li_2TiO_3 and different lithium-6 contents (7.6, 60 and 90 at%) were selected for the experiment. Material properties such as the chemical composition, phase content, microstructure, porosity, and mechanical properties were determined after certain time intervals and at the end of the experiment. The ACB pebbles show good performance under high temperatures as no lithium loss nor secondary phases occur. Furthermore, the microstructure, porosities, and mechanical stabilities did not exhibit significant changes over time.

Keywords: advanced ceramic breeder; long-term thermal stability; lithium orthosilicate + lithium metatitanate; lithium-6; fusion technology

1 Introduction

Advanced Ceramic Breeder (ACB) pebbles consist of the two phases lithium orthosilicate (Li_4SiO_4, LOS) and lithium metatitanate (Li_2TiO_3, LMT) and are fabricated using the KALOS process [1]. They represent the European Union's reference material for the ITER TBM and for the Helium Cooled Pebble Bed (HCPB) and the Water-cooled Lead Ceramic Breeder (WLCB) concepts in DEMO [2,3]. In the current HCPB DEMO design, the ACB pebbles have to withstand temperatures in the range from 400 to >900 °C [2]. For the alternative WLCB concept the temperature range will be similar (approx. 300–900 °C) [4]. Therefore, a comprehensive investigation of their thermal stability over a long time is necessary in order to evaluate the pebbles for their future use.

In the past, the long-term thermal stability of different ACB compositions (LOS + nominal 25, 30, 35 mol% LMT) was studied at 900 °C for up to 128 days in dry and slightly moist gas atmospheres (He + 0.1 vol% H_2 or H_2O) [5]. It was observed that the pebble samples remain

chemically stable without lithium loss over time. Only minor changes with regard to the microstructure occur and no significant grain growth was observed. Open and closed porosities remain stable over time. Crush load values decrease after one day of annealing most likely due to the phase transition from the cubic Li_2TiO_3 to the thermodynamically stable monoclinic Li_2TiO_3 crystal structure and its accompanying reordering of the structure, but also remains stable afterwards [5].

There also exist other studies on the thermal stability, but in most cases the chosen durations were usually significantly shorter. Examples for annealing experiments with comparable durations were performed at 970 °C in He + 0.1 vol% H_2 atmosphere for 96 days on Li_4SiO_4-, Li_2TiO_3- and Li_2ZrO_3-based pebble samples (all samples had an excess of SiO_2, TiO_2, and ZrO_2, respectively) [6-8]. The Li_4SiO_4-based pebbles were fabricated in a melt-spraying process [9], while the Li_2TiO_3 and Li_2ZrO_3 pebbles were produced using an extrusion-spheronisation method [10]. All samples showed no significant change in their lithium contents, but a certain decrease in their mechanical strengths. Some grain growth and a densification of the material was only observed for Li_2TiO_3 and Li_2ZrO_3 [6,8]. Ipponsugi et al. investigated Li_2TiO_3 pebbles fabricated by emulsion method with an excess of lithium after their heating at 900 °C for up to 1200 h (= 50 d) in Ar + 1 % H_2 atmosphere [11]. A lithium loss and grain growth were observed mainly within the first 240 h (= 10 d). Both properties did not show significant changes afterwards, which resulted in the conclusion that the grain growth is connected to the availability of evaporable lithium [11]. Moreover, the thermal stability of core-shell breeder materials was investigated by Gu et al. and Chen et al., consisting of a Li_4SiO_4 or Li_4TiO_4 core and a Li_2TiO_3 shell [12, 13]. For pebbles with a Li_4SiO_4 core and a Li_2TiO_3 shell a certain lithium loss after 1000 h at 900 °C in a He + 0.1vol% H_2 atmosphere is reported. It is assumed that the Li_2TiO_3 shell prevents the grain growth of the Li_4SiO_4 in the core. A decrease in the mean crush load values was observed after 100 h, but the values remained stable at a relatively high level in the following [12]. After 30 days in Ar + 1 % H_2 atmosphere the pebbles with a Li_4TiO_4 core and a Li_2TiO_3 shell show a total lithium mass loss of >3 %, as well as a significant grain growth in both, the core and the shell. The mechanical strength remained stable over time [13].

In the present study, long-term annealing (LTA) tests with ACB pebble batches enriched in lithium-6 were performed for the first time and directly compared to the long-term thermal performance of a sample without an enrichment in lithtium-6. An isotope effect on the material properties in general is not expected. However, in the case of a lithium evaporation, the lighter isotope lithium-6 might preferentially go into the gas phase.

2 Materials and Methods

2.1 ACB Samples

ACB pebbles were produced using the KALOS process [1]. One batch was produced using the raw materials (lithium hydroxide monohydrate ($LiOH{\cdot}H_2O$), silicon dioxide (SiO_2), and titanium dioxide (TiO_2)) with standard purity and no lithium-6 enrichment. Three batches were produced using raw materials with high purity and in addition $LiOH{\cdot}H_2O$ enriched in lithium-6 by 95 at% with a non-certified purity to obtain lithium-6 enrichments of 60 and 90 at% in the ACB pebbles. Moreover, the samples differ in their LMT-content having 30 or 35 mol% LMT. The sample names include their nominal LMT-content plus their nominal lithium-6 content at

the end, resulting in the following four samples: 30-LMT-90, 30-LMT-60, 35-LMT-60, and 30-LMT-7.6.

2.2 LTA Experiment

The LTA experiment was performed in a tube furnace that provides three individual alumina tubes that are heated simultaneously (see experimental setup in *fig. 1*). Gas composed of He + 0.1 vol% H_2 (as considered for the EU HCPB [2]) was streaming through each tube with a flow rate of 1200 ml_n/h. The pressure in the system was set slightly higher than ambient pressure (1200 mbar) to prevent air penetrating the system. Moisture sensors monitor the humidity at all gas effluent sides and at the common influent side. The oxygen content is measured by optical oxygen sensors at the influent side of tube 2 and the effluent side of all tubes.

Fig. 1. Schematic experimental set-up for the LTA experiment. Three tubes are included in the furnace that can be individually monitored with regard to their moisture and oxygen content and their pressure. During the experiment He gas including 0.1 vol% H_2 is flowing through the tubes.

All samples underwent the same temperature programme. Dwell times of 2, 20, 40, and 60 days (d) were used at the maximum temperature of 900 °C in a first run and of 700 °C in a subsequent second run. At the start of the experiment, tube 1 was loaded with the samples in alumina boats for 60 d and tube 2 was loaded with the samples for 20 d. After loading of the 20 d- and 60 d-samples, the temperature was first set to 300 °C for 20 h to remove the humidity inside the system, as well as the humidity that was introduced into the tubes while loading. Afterwards, the temperature was increased to 900 °C. Heating rates of 5 K/min were used. After 20 d, tube 2 was opened to retrieve the samples and the 40 d-samples were loaded. For sampling, the furnace was set to 300 °C due to safety reasons. As there is no active cooling possible, the cooling rate is about 0.5 K/min. After sampling the 40 d- and 60 d-samples, the 2 d-samples were loaded in tube 1. The shortest annealing time was put at the end to have the tubes as dry as possible as a possible influence would be higher for the very short dwell time. A scheme of the loading and sampling is shown in *figure 2*. Run 2 at 700 °C was started directly afterwards with the same loading and sampling scheme. The samples were loaded at 300 °C after retrieving the last samples of run 1 and the temperature was held for 20 h before raising the temperature to 700 °C. The temperature was monitored at each tube using thermocouples. Due to a limited amount of pebbles enriched in lithium-6, the amount was adjusted to their availability and for all samples, including the non-enriched one, about 6 g were used for each dwell time.

Fig. 2. Loading and sampling scheme of the LTA experiment; d = day, t = tube.

2.3 Analytical Methods

Chemical analysis was performed to measure the lithium, silicon, and titanium content using Inductively Coupled Plasma Optical Emission Spectrometry (ICP-OES; *iCAP 7600 CUO* by *Thermo Fisher Scientific*). Furthermore, the lithium isotope ratio was measured by Inductively Coupled Plasma Mass Spectrometry (ICP-MS; *Agilent 7500ce* by *Agilent Technologies*) considering a lithium carbonate standard. For each sample a triple determination was

performed; furthermore, a four-point calibration with a certified standard for each single element and scandium as an internal standard were used. Furthermore, the lithium-6 content of the pristine samples was measured at the *Bundesanstalt für Materialforschung (BAM)*, Germany, using a high resolution ICP-MS (*Element XR* by *Thermo Fisher Scientific*) and the reference material NIST RM8545 for lithium isotopes in lithium carbonate (LSVEC).

Finely ground pebbles were analysed with regard to their phase composition using powder X-ray diffraction (XRD; *D2 PHASER* diffractometer by *Bruker AXS*) with Cu-Kα in air (2 theta range = 10–85°, 0.02°/step, 1 s/step, 15 rpm). For all measurements a silicon low background sample holder was used. The following reference data was used to verify the occurring phases: Li_4SiO_4 (ICSD-25759, PDF-01-074-0307 [14]), m-Li_2TiO_3 (monoclinic, ICSD-15150, PDF-01-071-2348 [15]), c-Li_2TiO_3 (cubic, ICSD-261235, PDF-01-080-7159 [16]), $Li_6Si_2O_7$ (ICSD-25752, PDF-01-074-0300 [17]), and Li_2SiO_3 (ICSD-16626, PDF-01-072-1140 [18]).

Helium pycnometry (*AccuPyc® II* by *Micromeritics*) was used to measure the skeletal density of the ceramic pebbles, which was subsequently used to determine the closed porosity of the samples. Three measurements were performed for each sample. To determine the open porosity, mercury porosimetry was applied (*PASCAL 140/440 Evo porosimeter* by *Thermo Fisher Scientific*). To not include the open spaces in the pebble bed in the open porosity, a pre-filling with mercury at low pressure was applied before the actual measurement. For the pristine samples, three measurements were performed each while only one measurement was performed for the pebbles heat-treated at 900 °C for 60 days due to its very limited material amount.

Uniaxial crush load tests were performed to investigate the mechanical strength of the pebble samples. 40 pebbles (screened to a diameter of 1000 µm of each sample) were measured using a universal testing machine (*zwickiLine 5 kN, Xforce HP load cell 100 N, ZwickRoell*).

To investigate the microstructure, cross sections of the pebbles were analysed by Scanning Electron Microscopy (SEM) using a *Zeiss SUPRA 55 microscope* with a Secondary Electron (SE) detector. Numerous pebbles were embedded in epoxy resin and ground to about half of their size. Afterwards, the cross sections were etched with water to improve the distinction between the two phases and sputtered with a thin layer of noble metals (Au/Pd). For recording the SEM images an acceleration voltage of 10 kV and a working distance of about 10 mm were used.

3 Results and Discussion

3.1 Experimental conditions

The recorded temperatures of the first run at 900 °C and the second run at 700 °C are displayed in *figure 3*. It can be seen that the actual temperatures were slightly higher than the set maximum temperatures. As mentioned before, the temperature was reduced to 300 °C for loading and sampling (compare scheme in *fig. 2*).

Fig. 3. Temperature profiles for the LTA experiment at 900 °c (top) and at 700 °C (bottom) in the used furnace tubes t1 and t2.

All samples were annealed in an atmosphere of He + 0.1 vol.% H_2 gas. The set gas pressure stayed constant during the experiment within 1200±0.25 mbar. The humidity and oxygen

contents were constantly measured during the LTA experiment at the influent and effluent sides. Therefore, the humidity- and oxygen-release can be determined.

At the beginning of run 1, the oxygen release of both tubes was about 200,000 ppm_v (i.e. approximately the oxygen content in air) and reached after 0.5 d relatively constant levels of about 400 and 300 ppm_v in tube 1 and 2, respectively. When a tube was opened for sampling/loading, the oxygen release shortly (i.e. for 0.2–0.3 d) increased to about 70,000–80,000 ppm_v due to the introduction of air into the tube and dropped back to the before mentioned constant values. At the beginning of run 2, the oxygen release of both tubes was about 70,000 ppm_v. This corresponds to the values after shortly opening the tubes in run 1, because run 2 was started directly after run 1 was finished. Again, after about 0.5 d the values decreased to and remained at approximately 400 and 300 ppm_v in tube 1 and 2, respectively. Due to an opening of a tube, the oxygen release shortly increased to about 70,000–80,000 ppm_v and dropped back after a short time.

At the beginning of run 2, the water release was about 13,000 and 19,000 ppm_v in tube 1 and tube 2, respectively. The relatively high release of water in the beginning, results from the humidity in the air that is in the tube on the one hand, and also from the adsorbed water on the ACB pebbles (although they are stored in a dry atmosphere, they will adsorb a small amount of water when handled in air for the experiment). The water release dropped quickly and increased again when the temperature was changed from 300 to 900 °C. After 3 d (i.e. ~1 d at 900 °C), the values decreased to about 240 and 560 ppm_v, while the water release was about 40 and 160 ppm_v at the end of run 1 for tube 1 and tube 2, respectively. As air with a certain humidity was introduced during sampling/loading, the water release shortly (i.e. for ~0.5 d) rose to 9,000–16,000 ppm_v in the respective tube. At the beginning of run 2, the water release was about 9,000 and 11,500 ppm_v in tube 1 and tube 2, respectively. The water release is lower here – comparable to the oxygen release – as the second run was performed directly after the first run and the tubes were heated for longer time already. Again, the water release dropped and shortly increased again, when the temperature was raised from 300 to 700 °C. After 3 d (i.e. ~1 d at 700 °C), the values decreased to about 130 and 290 ppm_v, while the water release was about 30 and 180 ppm_v at the end of the experiment for tube 1 and tube 2, respectively.

3.2 Chemical and Phase Compositions

The actual LMT and lithium-6 contents of the samples used for the LTA experiment were determined within a chemical analysis using ICP-OES (at KIT) and ICP-MS (at BAM), respectively (see *table 1*). The LMT content is close to the nominal values and lies slightly below them, which is resulting from the fabrication process. The lithium-6 content is in good agreement with the nominal values for all samples.

Table 1. Li_2TiO_3 (LMT) analysed via ICP-OES at KIT and lithium-6 content analysed via ICP-MS at BAM of the samples used for the LTA experiment.

	30-LMT-90	**30-LMT-60**	**35-LMT-60**	**30-LMT-7.6**
LMT / mol%	28.4 ± 0.4	28.9 ± 0.4	32.7 ± 0.4	29.5 ± 0.3

Li-6 / at%	88.97 ± 0.04	61.3 ± 0.1	60.3 ± 0.1	7.5 ± 0.1

For the long-term thermal stability, it is important that the samples do not lose lithium. Therefore, the lithium content was determined after the different dwell times in the LTA experiment at 700 and at 900 °C (see *fig. 4*). Within the inaccuracy of the measurement the lithium mass remains stable. Therefore, all samples did not lose lithium over time at both temperatures.

Fig. 4. Development of the total lithium content and its measurement inaccuracy versus the dwell time for pebble samples annealed at 700 °C (left) and at 900 °C (right).

Furthermore, the lithium isotope ratio was measured after all dwell times to check if there was an effect on a specific isotope over time. The lithium isotope ratio (Li-6/Li-7) over time at both temperatures is displayed for all samples in *figure 5*. For the 30-LMT-90 sample the actual lithium isotope ratio lies below the nominal ratio of 90:10, while the actual ratios of the samples 30-/35-LMT-60 are slightly higher than 60:40 due to slight deviations from the nominal enrichments. It should be noted here that all values for the lithium isotope ratio over time were taken from measurements at KIT for better comparison among each other. Therefore, the values of the pristine samples (i.e. 0 d) differ slightly from the values determined by BAM (compare *table 1*). For the highly enriched sample 30-LMT-90 (see *fig. 5, left*), the values show no clear trend. For both annealing temperatures the values decrease after 2 d slightly. For the annealing at 700 °C the lithium isotope ratio increases and decreases again in the following, while for the annealing at 900 °C the values increase again. Although these variations are slightly outside of the measurement inaccuracy, these variations do not show a tendency of certain behaviour of one lithium isotope. For the samples with a nominal lithium-6 enrichment of 60 at% (see *fig. 5, right*), the lithium isotope ratios only vary slightly within the measurement inaccuracy. In addition, the lithium isotopes versus dwell time are plotted individually in *figure S1* in the *supplementary material*. Therefore, no effect with regard to a specific lithium isotope can be observed over time at elevated temperatures.

Fig. 5. Development of the lithium isotope ratio including its measurement inaccuracy versus the dwell time for pebble samples enriched in lithium-6 with 90 at% (left) and with 60 at% (right) at 700 °C (blue) and 900 °C (red).

**Figure 6* shows selected XRD patterns for all samples. For better clarity only XRD patterns of the pristine samples and after the shortest and the longest dwell time (2 and 60 d, respectively) at 900 °C are shown. In comparison, XRD patterns of the LTA experiment at 700 °C can be seen in *figure S2* in the *supplementary material*.

Fig. 6. Normalised XRD patterns for all samples comparing the pristine sample to samples annealed with the shortest (2 d) and the longest (60 d) dwell time at 900 °C. The main reflections of the phases are given as: Li_4SiO_4 (red), c-Li_2TiO_3 (cyan), m-Li_2TiO_3 (blue), $Li_6Si_2O_7$ (yellow), Li_2SiO_3 (green), and an unknown impurity is marked with an asterisk.

The pristine samples show in all cases the two main phases monoclinic Li_4SiO_4 and cubic Li_2TiO_3. The c-Li_2TiO_3 is metastable at room temperature and occurs due to the rapid cooling at the end of the KALOS process [1]. Already after short annealing times (here 2 d) the metastable c-Li_2TiO_3 is transformed to the m-Li_2TiO_3 phase stable at low temperatures. This is the case for both annealing temperatures, only that the crystallinity of the monoclinic Li_2TiO_3

is lower at 700 °C compared to the samples annealed at 900 °C (compare e.g. reflection peak at ~18.5° in *figs. 6 and S2*). The lower crystallinity should not be problematic as the shape of the LMT dendrites that stabilises the microstructure, is not influenced by this phase transition.

Sample 30-LMT-90 furthermore, shows impurities in the pristine sample. This is lithium pyrosilicate ($Li_6Si_2O_7$, the most intense reflection peak is marked in yellow in *fig. 6*) on the one hand and an unidentifiable phase (reflections marked with an asterisk in *fig. 6*) on the other hand. $Li_6Si_2O_7$ is depleted in lithium compared to LOS and was formed due to a slight Li-deficit during the weighing of the enriched $LiOH{\cdot}H_2O$ raw material. As $Li_6Si_2O_7$ is again a high-temperature phase resulting from the quenching during the fabrication process and exists only metastably at room temperature, it is transformed to lithium metasilicate (Li_2SiO_3, most intense reflection peak is marked in green in *fig. 6*) after the annealing. Again, the phase transformation takes place already after short time at elevated temperatures.

The XRD results underline the one from the chemical analysis that no significant lithium loss takes place over time, which would result in lithium depleted phases like Li_2SiO_3.

3.3 Microstructure

In general, two different types of microstructures can be found in ACB pebbles [5]. This is because the melt composition is not perfectly homogenous during the KALOS process. One type shows large LMT dendrites that form first and LOS grains that form in the spaces in between (cf. *fig. 7, top row*). The LOS is hardly visible in the SEM images as it is underlying the LMT dendrites due to the etching process in the preparation of the cross sections. This microstructure forms in a melt with a higher LMT content. However, melt with a lower LMT content leads to a microstructure with finer LMT dendrites and LOS grains that form in between (cf. *fig. 7, bottom row*). The finer dendrites have quite a variety of appearances, which makes a direct comparison difficult in some cases.

The development of the microstructure after the LTA at 700 and 900 °C was investigated in cross sections using SEM. *Figure 7* shows SEM images after all dwell times at 900 °C for the sample 30-LMT-90 as an example; further SEM images can be found in the *supplementary material* in *figures S3–S5*. Over the LTA duration no significant changes in both types of microstructure are observed. This is valid for both LTA temperatures and all four samples included in the study.

Fig. 7. Development of the two different types of microstructure exemplary for the sample 30-LMT-90 at 900 °C.

After the LTA, still large LMT dendrites are observed as in the pristine sample. Also, the microstructure exhibiting the smaller LMT dendrites is observed as it occurs in the pristine sample. Nevertheless, and as aforementioned, a direct comparison is slightly more difficult as the variety of this type of microstructure is higher. In a previous study it was described that the smaller dendrites in comparable compositions (i.e. 30 and 35 mol% LMT) partly changed to spherical grains over the annealing time [5]. The current observations cannot underline this. Although, also microstructures with more spherical grains of LMT are observed, this microstructure is not only found after different LTA dwell times, but also in the pristine sample. This is part of the mentioned variety of this microstructure type. Therefore, the assumption from [5] cannot be validated and may even need to be corrected. Within the current study more SEM images were taken, which could have led to a clearer picture. A

significant change in the microstructure including a transformation to more spherical grains over time at elevated temperatures cannot be constituted for the ACB pebbles with an LMT content of 30 and 35 mol%. It is hard to analyse the development of grain growth as the microstructure is quite diverse and the LOS grains often underlie the LMT dendrites in the etched cross sections. As far as detectable, no significant grain growth took place in the biphasic material.

3.4 Porosities

The closed porosities were derived from the measured skeletal densities and the theoretical densities. The values for closed porosities versus the dwell time at 700 and 900 °C are displayed in *figure 8*. Already after production, the ACB pebble batches enriched in lithium-6 have higher closed porosities with a mean value of 3.9±0.3 % compared to the non-enriched sample with 1.5±0.2 %. In principle, an influence of the different $LiOH \cdot H_2O$ raw materials (Li-6 enriched vs. non-enriched) is not expected as the powders were melted during the fabrication process. However, it cannot completely be excluded. For the sample with natural lithium-6 abundance 30-LMT-7.6, no change in the closed porosity is observed as the values remain constant with a mean value of 1.4±0.2 % during the annealing. For the samples enriched in lithium-6 30-LMT-90, 30-LMT-60, 35-LMT-60, the closed porosity values appear to decrease after 2 d of annealing and remain stable afterwards with an overall mean value of 2.9±0.4 %. However, this decrease is 1 percentage point (pp), which corresponds to the estimated error of measurement. Therefore, no obvious trend can be observed with regard to the closed porosity over time at both temperatures for all samples. For the sample not enriched in lithium-6, no decrease of the closed porosity is observed.

Fig. 8. Development of the average closed porosity and its standard deviation versus dwell time for pebble samples annealed at 700 °C (left) and at 900 °C (right). The measurement inaccuracy is estimated to be about 1 pp.

The open porosity was tested for the pristine pebbles and the pebbles annealed for 60 d at 900 °C to check its development. The open porosity in the pristine samples range from 0.9 to 2.6 % and after 60 d from 1.6 to 2.1 %. The sample with the highest LMT content 35-LMT-60 shows the lowest open porosity values. Within the estimated error of measurement (i.e. approx. 1 pp), no change in the open porosity values after the annealing at 900 °C was observed.

3.5 Mechanical Stability

To investigate the mechanical stability over time, crush load tests were performed. The results for pebbles with a diameter of 1000 µm are plotted in *figure 9* for both annealing temperatures.

Fig. 9. Development of the average crush load and its standard deviation versus the dwell time for pebbles (Ø = 1000 µm) annealed at 700 °C (left) and at 900 °C (right).

As LMT is the strengthening phase, the crush loads are generally higher the higher the LMT content. Here, the pristine sample 35-LMT-60 shows the highest crush load with 32±11 N. Still, the crush load values of the samples with nominal 30 mol% LMT are not much lower. Considering the actual LMT contents (cf. *table 1*), the crush loads follow the expected trend for the pristine samples: 35-LMT-60 > 30-LMT-7.6 > 30-LMT-60 > 30-LMT-90.

In general, the variation of the crush load values is relatively high resulting in a high standard deviation. Still, it can be deduced that the crush load values decrease for all samples after annealing at both temperatures after two days and remain more or less stable afterwards. The transformation from the high-temperature c-Li_2TiO_3 phase to the thermodynamically stable m-Li_2TiO_3 phase takes place after short time of the annealing. This goes along with a significant increase in the cell volume. Therefore, the decrease in crush load values is most likely due to reordering processes in the structure due to the phase transition. The decrease in crush load values for samples annealed at 700 and 900 °C was about 25–39 % and about 18–26 %, respectively. From the XRD analysis it can be seen that the crystallisation of the m-Li_2TiO_3 phase at 700 °C was not as good as at 900 °C. Also reordering processes in the structure might have been impeded too, which could explain the higher decrease in crush loads for samples annealed only at lower temperatures. In previous LTA experiments, also a decrease in the crush load values was observed. Pebbles with a diameter of 1000 µm that were annealed at 900 °C decreased by about 20–30 % in their crush loads after 1 d [5], which is in good agreement with the present study.

4 Conclusions

This LTA experiment was performed to investigate the thermal stability of ACB pebbles, and in particular pebbles enriched in lithium-6, at elevated temperatures over time. Four different batches of ACB pebbles were selected with LMT contents of 30 and 35 mol% and lithium-6 abundances of 7.6, 60 and 90 at%. The samples were tested at 700 and 900 °C in He + 0.1 vol% H_2 gas atmosphere for up to 60 d. The material remains chemically stable as no lithium loss nor the formation of secondary phases were detected over time. After the shortest dwell time of 2 d, LMT transforms into its monoclinic structure type, because the cubic Li_2TiO_3 formed during the pebble production is only metastable. The crystallinity of the formed monoclinic Li_2TiO_3 is higher in pebbles annealed at 900 °C compared to pebbles annealed at 700 °C. This lower crystallinity should not be problematic as the shape of the LMT dendrites that stabilises the microstructure and hence the material, is not affected by this phase transition. All four batches show the characteristic microstructures, which reveal no noticeable change over the annealing time. Hence, the biphasic ACB material with its distinctive LMT dendrites exhibits a stable microstructure at elevated temperatures. With regard to the closed porosity, the values of the sample with natural lithium-6 abundance with a mean value of 1.4±0.2 % are slightly lower in comparison to the three samples with an enrichment in lithium-6 (Ø = 3.1±0.5 %). While for the non-enriched sample no change in the porosity values is observed, the samples enriched in lithium-6 show a slight decrease of 1 pp after 2 d of annealing, although this still lies in the range of the measurement error. The development of the open porosity could only be tested on a selected number of samples at 900 °C and did not show a change outside the measurement error over time. After a decrease in crush load values after 2 d of annealing at 700 and 900 °C by about 25–39 % and about 18–26 %, respectively, the values remain stable over time. The decrease can be explained by the phase transition from cubic to monoclinic Li_2TiO_3 and accompanied by an increase in the cell volume of the crystal structure.

Ceramic breeder pebbles enriched in lithium-6 were used for the first time in thermal annealing experiments. No influence nor deteriorated material properties due to higher lithium-6 contents were observed in the performance of the ACB pebbles at elevated temperatures.

This work contributes to the understanding of the ceramic breeder material and its performance under harsh conditions in a future fusion reactor. The ACB material has high long-term thermal stability over time at temperatures of 700 and 900 °C. Still, it should be noted that the investigation of the long-term thermal stability covers only one important aspect of diverse challenges. Influences such as radiation damages or the formation of secondary phases due to a constant lithium burn-up were not covered in this study.

Acknowledgements

The authors thank Andra Lerghievici and Christina Odemer for the experimental support. Furthermore, the authors acknowledge the ICP-MS measurements of the lithium-6 enriched samples performed at BAM by Jochen Vogl. This work has been carried out within the framework of the EUROfusion Consortium, funded by the European Union via the Euratom Research and Training Programme (Grant Agreement No 101052200 — EUROfusion). Views and opinions expressed are however those of the author(s) only and do not necessarily reflect those of the European Union or the European Commission. Neither the European Union nor the European Commission can be held responsible for them.

References

[1] O. Leys, J.M. Leys, R. Knitter, Current status and future perspectives of EU ceramic breeder development, Fusion Eng. Des. 164 (2021) 112171; https://doi.org/10.1016/j.fusengdes.2020.112171.

[2] G. Zhou and F.A. Hernández, Current design of the EU DEMO Helium Cooled Pebble Bed breeding blanket, Proceedings of the 15th International Workshop on Beryllium Technology (BeWS-15) September, 14–15, 2022, Karlsruhe, Germany; https://doi.org/10.5445/IR/1000160101.

[3] G. Zhou, Y. Lu, F.A. Hernández, A water cooled lead ceramic breeder blanket for European DEMO, Fusion Eng. Des. 168 (2021) 112397; https://doi.org/10.1016/j.fusengdes.2021.112397.

[4] S. Giambrone, I. Catanzaro, G. Bongiovì, P.A. Di Maio, E. Vallone, P. Arena, F.A. Hernández, I. Moscato, G.A. Spagnuolo, P. Chiovaro, M. Giardina, A. Quartararo, E. Tomarchio, Preliminary thermo-mechanical assessment of the Top Cap region of the Water-Cooled Lead-Ceramic Breeder Breeding Blanket alternative concept, Fusion Eng. Des. 200 (2024) 114201; https://doi.org/10.1016/j.fusengdes.2024.114201.

[5] J.M. Heuser, M.H.H. Kolb, T. Bergfeldt, R. Knitter, Long-term thermal stability of two-phased lithium orthosilicate/metatitanate ceramics, J. Nucl. Mater. 507 (2018) 396–402; https://doi.org/10.1016/j.jnucmat.2018.05.010

[6] J.G. van der Laan, H. Kawamura, N. Roux, D. Yamaki, Ceramic breeder research and development: progress and focus, J. Nucl. Mater. 283–287 (2000) 99–109; https://doi.org/10.1016/S0022-3115(00)00352-4.

[7] J.D. Lulewicz, N. Roux, G. Piazza, J. Reimann, J. van der Laan, Behaviour of Li_2ZrO_3 and Li_2TiO_3 pebbles relevant to their utilization as ceramic breeder for the HCPB blanket, J.

Nucl. Mater. 283–287 (2000) 1361–1365; https://doi.org/10.1016/S0022-3115(00)00298-1.

[8] G. Piazza, J. Reimann, E. Günther, R. Knitter, N. Roux, J.D. Lulewicz, Behaviour of ceramic breeder materials in long time annealing experiments, Fusion Eng. Des. 58–59 (2001) 653–659; https://doi.org/10.1016/S0920-3796(01)00517-8.

[9] W. Pannhorst, V. Geiler, G. Räke, B. Speit, D. Sprenger, Production process of lithium orthosilicate pebbles, Proceedings of the 20th Symposium on Fusion Technology (SOFT-20) 7–11 September, 1998, Marseilles, France.

[10] J.D. Lulewicz and N. Roux, Fabrication of Li_2TiO_3 pebbles by the extrusion-spheronisation-sintering process, J. Nucl. Mater. 307–211 (2002) 803–806; https://doi.org/10.1016/S0022-3115(02)00981-9.

[11] A. Ipponsugi, K. Katayama, T. Hoshino, Li mass loss and structure change due to long time heating in hydrogen atmosphere from Li_2TiO_3 with excess Li, Nucl. Mater. Energy 25 (2020) 100777; https://doi.org/10.1016/j.nme.2020.100777.

[12] S. Gu, B. Ji, C. Wang, Q. Qi, H.-S. Zhou, Y. Zhang, G.-N. Luo, Effects of long-term high temperature annealing on Li_2TiO_3 and advanced core-shell Li_2TiO_3-Li_4SiO_4 tritium breeders, J. Nucl. Mater. 590 (2024) 154895; https://doi.org/10.1016/j.jnucmat.2023.154895.

[13] R. Chen, A. Ipponsugi, R. Oyama, J. Qi, H. Wang, Z. Huang, H. Guo, T. Lu, W. Feng, K. Katayama, Long-term thermal stability of Li_4TiO_4–Li_2TiO_3 core–shell breeding pebbles under continuous heating in H_2/Ar atmosphere, Int. J. Appl. Ceram. Tec. 20 (2023) 2576–2585; https://doi.org/10.1111/ijac.14392.

[14] H. Völlenkle, A. Wittmann, H. Nowotny, Die Kristallstruktur von Li_4SiO_4, Monatsh. Chem. / Chem. Monthly 99 (1968) 1360–1371; https://doi.org/10.1007/BF00902680.

[15] J.F. Dorrian and R.E. Newnham, Refinement of the structure of Li_2TiO_3, Mater. Res. Bull. 4 (1969) 179–183; https://doi.org/10.1016/0025-5408(69)90054-3.

[16] A. Laumann, K.T. Fehr, H. Boysen, M. Hölzel, M. Holzapfel, Temperature-dependent structural transformations of hydrothermally synthesized cubic Li_2TiO_3 studied by in-situ neutron diffraction, Z. Kristallogr. / Cryst. Mater. 226 (2011) 53–61; https://doi.org/10.1524/zkri.2011.1286.

[17] H. Völlenkle, A. Wittmann, H. Nowotny, The crystal structure of $Li_6[Si_2O_7]$, Monatsh. Chem. / Chem. Monthly 100 (1969) 295–303; https://doi.org/10.1007/BF00938267.

[18] H. Seemann, Die Kristallstruktur des Lithiummetasilikates, $(Li_2SiO_3)_x$, Acta Crystallogr. 9 (1956) 251–252; https://doi.org/10.1107/S0365110X56000693.